

1 **Effective removal of enteric viruses by *Moringa oleifera* seed extract functionalized**  
2 **cotton filter**

3  
4 **Authors**

5 Chamteut Oh<sup>\*,1,2)</sup>, Gang Zheng<sup>\*,1)</sup>, Laxmicharan Samineni<sup>3)</sup>, Manish Kumar<sup>4)</sup>, Thanh H.  
6 Nguyen<sup>1,5)</sup>

7  
8 \*Equal contribution

9 Corresponding author: Chamteut Oh (chamteutoh@ufl.edu)

- 10  
11
- 12 1) Department of Civil and Environmental Engineering, University of Illinois Urbana-  
13 Champaign, United States
  - 14 2) Department of Environmental Engineering Sciences, University of Florida, United  
15 States
  - 16 3) Department of Chemical Engineering, The University of Texas at Austin, Austin, USA
  - 17 4) Department of Civil, Architectural and Environmental Engineering, The University of  
18 Texas at Austin,
  - 19 5) Institute of Genomic Biology, University of Illinois Urbana-Champaign, United States
- 20  
21

22  
23  
24  
25  
26  
27  
28  
29  
30  
31  
32  
33  
34  
35

## Abstract

Accessible and low-cost point-of-use technologies have significant potential to mitigate risk to public health, particularly in areas with limited resources and in disaster scenarios. Natural cotton fibers functionalized with water-soluble proteins from *Moringa oleifera* seeds (*MO*-cotton filter) are a promising technology at lab-scale with demonstrated feasibility for pathogen removal from water. Here, we showed the performance of *MO*-cotton filters under practically relevant conditions to remove mammalian virus spiked in groundwater. Specifically, *MO*-cotton filters achieved  $> 3.2\text{-log}_{10}$  reduction at a superficial velocity of 0.7 m/h of two mammalian viruses Tulane virus (TV, *Caliciviridae*, non-enveloped virus) and Transmissible gastroenteritis virus (TGEV, *Coronaviridae*, enveloped virus), which are representative of a significant portion of waterborne illnesses. We further evaluated the risk of virus particles detached due to shear forces by testing their infectivity and found that the viruses accumulated on the *MO*-cotton filters pose a minimal risk of contaminating the drinking water source.

## 36 **Introduction**

37 Enteric viruses are a significant cause of waterborne diseases and acute diarrhea, resulting in  
38 approximately 1.7 billion infections and 525,000 deaths in children under the age of 5 years  
39 annually <sup>1</sup>. Unfortunately, enteric viruses disproportionately affect the health of individuals  
40 belonging to low socioeconomic status <sup>2,3</sup>. For instance, approximately 90% of diarrhea related  
41 deaths occur in sub-Saharan Africa and South Asia, where there is lack of access to appropriate  
42 water, sanitation, and hygiene (WASH) <sup>4</sup>. As a result, point-of-use (POU) water treatment  
43 technologies have been studied as a cost-effective decentralized solution <sup>5</sup>. However, many  
44 POU water treatment technologies have not achieved sustained use at the household level  
45 because they require operational knowledge, such as chemical dose for chlorination, or rely on  
46 less accessible materials. For instance, only 1.5% of households in low- and middle-income  
47 countries, that received training to operate coagulant-chlorine disinfection systems,  
48 appropriately treat their drinking water after 6 months <sup>5</sup>.

49 Due to the low cost, simple maintenance, high treatment capacity, and high  
50 performance against a wide variety of contaminants, filtration has been identified as a  
51 promising point-of-use (POU) water treatment technology. POU filters have the potential to be  
52 widely adopted sustainably in low- and middle-income countries, to improve the household  
53 water quality and reduce the risk of waterborne diseases and deaths <sup>6-8</sup>. However, a primary  
54 challenge associated with conventional filtration technologies, such as sand and ceramic filters,  
55 is their inability to effectively filter viruses <sup>7,9</sup>. For instance, rapid sand filtration achieved only  
56 a 1.26- $\log_{10}$  reduction for pepper mild mottle virus and a 0.49- $\log_{10}$  reduction for JC  
57 polyomavirus <sup>10</sup>. Similarly, ceramic filters were unable to achieve even a 1- $\log_{10}$  reduction of  
58 MS2 virus <sup>11,12</sup>. Given that viral pathogens are one of the primary causes of waterborne diseases  
59 <sup>13</sup>, there is an urgent need for POU water filtration technologies that can effectively reduce the  
60 risk of water-borne viral infections.

61           Recent studies have focused on enhancing the virus removal effectiveness of filtration  
62 technology by functionalizing the surface of a filter media with easily accessible natural  
63 materials. *Moringa oleifera* (*MO*), a fast-growing deciduous tree found in tropical regions, has  
64 garnered attention due to its ability to thrive in areas facing significant challenges in obtaining  
65 safe drinking water<sup>14</sup>. A water extract containing cationic proteins, derived from *MO* seeds can  
66 functionalize filter media and adsorb viruses that are typically negatively charged in the  
67 environment<sup>14</sup>. In our previous research, we successfully functionalized model sand particles  
68 with the moringa proteins and demonstrated a virus removal efficacy of up to a 7-log<sub>10</sub> using  
69 MS2 bacteriophage as a model virus<sup>15</sup>. However, the challenges associated with low filter  
70 loading rate and the availability of appropriately sized natural sand grains (<130 μm) have  
71 necessitated the exploration of alternative filter media. Subsequently, we have shown that  
72 natural cotton can be successfully functionalized with *MO* seed extract (*MO*-cotton filters),  
73 creating an affinity-based filter for the removal of contaminants from water which shows  
74 exceptional virus, bacteria, and inorganic nanoparticle removal<sup>16,17</sup>. Despite the promising  
75 performance at lab-scale, research on *MO*-cotton filters to date involved the use of surrogate  
76 virus, MS2 bacteriophage, deionized water with additives like NaCl as artificial water matrix  
77 and has been conducted over a relatively short duration. These experimental conditions lack  
78 representation of the real-world application scenario for *MO*-cotton filters where consistent  
79 virus removal against mammalian viruses over long periods of operation is required limiting  
80 the wide application of *MO*-cotton filters in the field.

81           This study aims to evaluate the effectiveness of *MO*-cotton filters in removing enteric  
82 viruses under real-world conditions. Specifically, we focused on two mammalian viruses: the  
83 Tulane virus (TV, rhesus monkey virus) and transmissible gastroenteritis virus (TGEV, porcine  
84 virus) as representative viral species belonging to the *Caliciviridae* and *Coronaviridae*,  
85 respectively. These viruses are responsible for a significant portion of waterborne illnesses

86 worldwide, including diarrhea<sup>18,19</sup>. In addition, viruses are categorized into enveloped or non-  
87 enveloped viruses depending on the presence or absence of an encapsulating lipid bilayer  
88 membrane. Therefore, TGEV (an enveloped virus) and TV (a non-enveloped virus) have been  
89 selected intentionally for this study to represent the behavior of a variety of viral pathogens in  
90 the environment. Furthermore, the virus removal efficacy of the *MO*-cotton filters was  
91 determined by experiments using actual groundwater spiked with these mammalian viruses,  
92 creating conditions that closely resemble real-world scenarios. Through column experiments  
93 and systematic analyses, we investigated the kinetics of virus removal and determined the fate  
94 of viruses during the filtration processes. The risk of detached viruses from *MO*-cotton filters  
95 was also studied here as this is a critical factor for ensuring safety of public health. Virus  
96 detachment experiments were conducted by operating the *MO*-cotton filters at high superficial  
97 velocity and simulating high shear conditions in batch experiments. Our results showed that  
98 even when operated at a superficial flow velocity (2.1 m/h) that is three times higher than the  
99 filtration rate, no detectable viruses were released from the filter (i.e., < 2.1 gene copies/ $\mu$ L).  
100 Viruses detached from the filter by a strong shear force in batch experiments were also  
101 confirmed to be inactivated by the moringa protein-induced aggregation. These results  
102 demonstrate that *MO*-cotton filters can effectively remove viruses from groundwater, thereby  
103 contributing to the mitigation of waterborne diseases through their use in POU filters.

104

## 105 **Materials and Methods**

### 106 **Moringa protein functionalized cotton filter preparation**

107 *Moringa oleifera* seeds were obtained from Echo Global Farms (USA). One gram of seed was  
108 weighed and crushed to a fine powder using a grinder for about 10 seconds. The ground seed  
109 was then mixed with 50 mL of deionized (DI) water at 100 rpm for 15 minutes to extract  
110 proteins. The well-mixed moringa seed extract was filtered through a 0.22  $\mu$ m filter to remove

111 the seed debris. Next, 1.75 g of cotton was weighed and soaked in DI water for approximately  
112 10 minutes to prevent air entrapment. The dampened cotton was then packed into a clean  
113 column with an inner diameter of 1.5 cm and a height of 10 cm (7374151, Bio-Rad, USA). The  
114 column was secured with an adaptor (7380016, Bio-Rad, USA). The cotton filled 4 cm of the  
115 column, corresponding to a volume of 7.1 cm<sup>3</sup>. Deionized (DI) water was first pumped to flow  
116 through the column filter at a rate of 2 mL/min for 30 minutes to saturate the cotton filter with  
117 water. Then, 50 mL of the filtered moringa extract was flowed through each column at 2  
118 mL/min for 25 minutes to coat the cotton fiber with moringa proteins. The total protein  
119 concentrations of influent and effluent were measured using Quick Start™ Bradford Protein  
120 Assay Kit 2 (Bio-Rad, USA) following the manufacturer's protocol to determine the protein  
121 amount coated on the cotton fiber. **Fig. S1** shows that the total protein concentration of the  
122 effluents was saturated to that of the initial solution, indicating the cotton filter was  
123 functionalized by the moringa proteins within 25 minutes. Note that this in situ coating method  
124 was found to be more efficient compared to the batch process <sup>15</sup>.

125

### 126 **Propagation of testing viruses**

127 TV and TGEV were provided by the Cincinnati Children's Hospital Medical Center <sup>20</sup> and the  
128 Veterinary Diagnostic Laboratory at the University of Illinois Urbana-Champaign, respectively  
129 (Oh et al., 2022a). We sequenced 6 kilo-bases (kb) of the TV genome and 10 kb of the TGEV  
130 genome, which are similar to the sequences of TV (99% identity with NC\_043512.1) and  
131 TGEV (99% identity to KX900394.1) in the GenBank (Fuzawa et al., 2019 and Supplementary  
132 file 1). This finding confirmed the identity of the virus stocks used in this study. We propagated  
133 the TV and TGEV in MA 104 (CRL-2378.1, ATCC, USA) and ST cell lines (CRL-1746,  
134 ATCC), respectively, supplemented by a complete culture medium. The complete culture  
135 medium consisted of 1X minimum essential medium (MEM; Thermo Fisher Scientific, USA),

136 2% fetal bovine serum (FBS; Thermo Fisher Scientific, USA), 1X antibiotic-antimycotic  
137 (Thermo Fisher Scientific, USA), 17 mM NaHCO<sub>3</sub>, 10 mM HEPES, and 1 mM sodium  
138 pyruvate (Thermo Fisher Scientific, USA). The cells were incubated at 37°C with 5% CO<sub>2</sub> for  
139 2 days. Following incubation, the viruses were released from their host cells through three  
140 cycles of freeze and thaw. Centrifugation at 2000 rpm (556 g) for 10 minutes using a Sorvall  
141 Legend RT Plus centrifuge (Thermo Fisher Scientific, MA, USA) was employed to separate  
142 the viruses from the cell debris. The resulting supernatant was filtered using a 0.22 µm filter  
143 (Millipore Sigma, MA, USA) and stored in 1 mL aliquots as stock solutions at -80°C until  
144 further use.

145

#### 146 **Viral RNA quantification**

147 Viral RNA was extracted from samples using the QIAamp Viral RNA mini kit (Qiagen,  
148 Germany), following the manufacturer's instructions. The extracted viral RNA was stored at -  
149 30°C and analyzed using reverse transcriptase quantitative polymerase chain reaction (RT-  
150 qPCR) within three days. The RT-qPCR mixture included 3 µL of RNA sample, 0.3 µL of 10  
151 µM forward primer, and 0.3 µL of 10 µM reverse primer, 1.275 µL of molecular biology grade  
152 water (Corning, NY, USA), 5 µL of 2×iTaQ universal SYBR green reaction mix, and 0.125 µL  
153 of iScript reverse transcriptase from the iTaq™ Universal SYBR® Green One-Step Kit  
154 (1725151, Bio-Rad Laboratories, USA). The RT-qPCR mixture was dispensed in 96-well  
155 plates (4306737, Applied Biosystems, USA) and analyzed by an RT-qPCR system  
156 (QuantStudio 3, Thermo Fisher Scientific, USA). The RT-qPCR mixture was incubated with a  
157 thermocycle of 50°C for 10 minutes, 95°C for 1 minute, and then 40 cycles of denaturation at  
158 95°C for 10 seconds, annealing and extension at 60°C for 30 seconds. Melting curves were  
159 analyzed while the temperature increased from 60°C to 95°C at the end of each RT-qPCR  
160 analysis. No primer-dimers were detected in any of the RT-qPCR analyses. The SYBR signal

161 was normalized to the ROX reference dye. The cycles of quantification (Cq) were determined  
162 by QuantStudio Design & Analysis Software (v1.5.1). Each RT-qPCR mixture, including  
163 synthetic DNA for a standard curve (and a positive control), molecular biology grade water as  
164 a negative control, and the viral RNA samples, was analyzed in at least three technical  
165 replicates. The linear dynamic range for the serial dilutions of synthetic DNA ranged from  $10^0$   
166 to  $10^5$  gene copies (gc)/ $\mu\text{L}$ . The PCR efficiencies for the RT-qPCR assays were above 85%  
167 ( $R^2 > 0.99$ ). The details of the RT-qPCR assays are summarized in **Table S1 and S2**, adhering  
168 to the MIQE guidelines<sup>22</sup>. An inhibition test was conducted by adding 1  $\mu\text{L}$  of  $10^3$  gc/ $\mu\text{L}$  bovine  
169 coronavirus RNA (BCoV; Merck Animal Health, USA), which is not expected to exist in our  
170 groundwater samples, to 10  $\mu\text{L}$  of RNA extract and 10  $\mu\text{L}$  of molecular biology grade water.  
171 We found that the differences in Cq values for BCoV RNA between the RNA extract and the  
172 water were smaller than 1, meaning that the impact of any possible inhibitors was negligible  
173 (**Fig. S2**) (Oh et al., 2022b). The limit of detection (LOD) for the RT-qPCR assays for TV and  
174 TGEV was determined using 20 replicates of serial dilutions of synthetic DNA controls (Oh et  
175 al., 2022b). We found that the LODs for TV and TGEV were  $2.14 \times 10^3$  and  $8.91 \times 10^2$  gc/mL,  
176 equivalent to 2.1 and 0.9 gc/ $\mu\text{L}$ , respectively (**Fig. S3**).

177

## 178 **Column experiments**

179 A schematic illustration for column experiments conducted is depicted in **Fig. 1A**. The virus  
180 stock solution of either TV or TGEV was diluted 1000-fold in autoclaved groundwater,  
181 obtained from the Newmark building at the University of Illinois Urbana-Champaign. The TV-  
182 containing groundwater included TV RNA concentrations of  $10^{6.6}$  gc/mL, and the TGEV-  
183 containing groundwater had TGEV RNA concentrations of  $10^{5.2}$  gc/mL. The virus-containing  
184 groundwater was continuously pumped into the *MO*-cotton filter. The flow rate of the virus-  
185 containing groundwater was set to 2 mL/min and adjusted for the constant flow rate throughout



186 the virus removal experiments. The influent and effluent were sampled over time to evaluate  
187 the virus removal efficacy of the *MO*-cotton filters. RNA concentrations of the influent were  
188 not significantly reduced throughout the virus removal experiments ( $p > 0.05$  from a linear  
189 regression analysis, **Fig. S4**), meaning the natural inactivation was negligible. Log virus  
190 reduction value was determined by RNA concentrations of influent divided by that of effluent  
191 on a log scale (i.e.,  $\text{Log}_{10} C_{\text{influent}}/C_{\text{effluent}}$ ). Virus removal efficacy was evaluated by presenting  
192 the log virus reduction values with a normalized time scale, dimensionless column volumes  
193 (CV) (**Eq. 1**).

194

$$195 \quad CV = \frac{\text{elapsed time (min)} \times \text{flow rate (mL/min)}}{\text{column volume occupied with cotton (mL)}} \quad (\text{Eq. 1})$$

196

197 Because the flow rate and column volume were set to 2 mL/min and 7.1 mL, respectively, 3.5  
198 minutes of elapsed time was equal to 1 CV. Virus removal kinetics was determined by two  
199 non-linear regression models, Thomas (**Eq. 2**) and Logarithm models (**Eq. 3**).

200

$$201 \quad \text{Log}_{10}\left(\frac{gC_{\text{influent}}}{gC_{\text{effluent}}}\right) = \text{Log}_{10}(1 + \exp(a + bCV)) \quad (\text{Eq. 2})$$

$$202 \quad \text{Log}_{10}\left(\frac{gC_{\text{influent}}}{gC_{\text{effluent}}}\right) = \text{c} \ln(CV) + d \quad (\text{Eq. 3})$$

203

204 where,  $gC_{\text{influent}}$  and  $gC_{\text{effluent}}$  indicate RNA concentrations of influent and effluent, CV is  
205 column volumes, normalized time term (**Eq. 1**), and a, b, c, d are constants. The Thomas model  
206 is one of the most widely used to describe breakthrough curves of the fixed-bed column<sup>23,24</sup>  
207 and the logarithmic model has been used to describe contaminant removal efficacy in filtration  
208 systems<sup>25–27</sup>.

209

210

### 211 **Quantification of risk from detached virus particles**

212 In addition to evaluating the virus removal efficiency of *MO*-cotton filters, we also conducted  
213 virus detachment experiments, designed to investigate the potential detachment of viruses  
214 accumulated on the *MO*-cotton filters. Detachment of viruses was induced by two methods in  
215 this study. After the TV removal experiments described above were completed, we flowed  
216 sterilized groundwater (i.e., no viruses were spiked) at a flow rate of 6 mL/min for about 30  
217 minutes to induce virus detachment at high superficial velocity. Furthermore, one-third of the  
218 cotton on the top was taken from the column and transferred to a sterilized 50 mL tube. We  
219 added 10 mL of DI water and vortexed the mixture for 2 minutes, incubated at room  
220 temperature for 10 min, and then vortexed for 2 minutes again to simulate high shear conditions  
221 and detach viruses from the cotton fiber. After detachment was induced, the infectious TV titer  
222 and TV RNA concentrations of the effluent solution were quantified as described below to  
223 evaluate the risk of detached viruses.

224

### 225 **Infectious virus titer measurement**

226 Plaque assays were conducted to determine infectious virus titers of TV and TGEV, following  
227 the protocol described by Oh et al. (2022a). A monolayer of MA104 and ST cells was prepared  
228 in the complete culture medium. The plaque assay was performed when the cell confluency  
229 reached approximately 100% on 6-well plates (USA Scientific, USA). For the plaque assay,  
230 each virus sample was serially diluted 10-fold in the complete culture medium without 10%  
231 FBS. Subsequently, 800  $\mu$ L of each serial dilution was added to each well of 6-well plates and  
232 incubated for 1 hour at 37°C with 5% CO<sub>2</sub>. After 1 hour, the supernatants were aspirated, and  
233 a 2 mL overlay solution consisting of 1X MEM, 1% agarose, 7.5% sodium bicarbonate, 15  
234 mM HEPES, and 1X antibiotic-antimycotic was added to the cellular monolayers. The overlay

235 solution was solidified by incubating at 4°C for 20 minutes. After a 2-day incubation at 37°C  
236 with 5% CO<sub>2</sub>, the 2 mL of a 10% formaldehyde solution was added to each well and incubated  
237 at room temperature for approximately 1 hour. Finally, the overlay and formaldehyde solution  
238 were removed, and the plaques were visualized by adding 0.5 mL of 0.05% crystal violet dye  
239 solution. Plaque-forming units (PFU) were counted over a lightbox. One PFU on a well with  
240 an 800 µL 10-fold dilution of the original sample represented the lowest infectious virus titer.  
241 As a result, the limit of detection (LOD) for the plaque assays was 10<sup>1.1</sup> PFU/mL in this study.

242

### 243 **Batch experiments**

244 Interactions between moringa proteins and TV were investigated through batch experiments to  
245 understand the mechanism of inactivation for viruses on *MO*-cotton filters. Schematic  
246 illustration for the batch experiment is depicted in **Fig. 3A**. Groundwater was spiked with TV  
247 to achieve a final RNA concentration of 10<sup>6.1</sup> gc/mL. A total of 675 µL of the TV-containing  
248 groundwater was then mixed with 75 µL of moringa proteins, with varying total protein  
249 concentrations ranging from 0 to 25.3 mg/mL. After a 5-minute reaction period, 750 µL of FBS  
250 was added to stop the reactivity of the moringa proteins. Subsequently, the final reactants were  
251 examined for infectious TV titers, total TV RNA, and TV aggregates. The TV aggregates were  
252 analyzed according to the aggregation assay described in the subsequent methods. Note that  
253 **Fig. S5** represents that FBS-quenched moringa proteins did not cause a significant impact on  
254 infectious TV titers compared to that of PBS, indicating that FBS can quench the moringa  
255 protein activity under our experimental conditions.

256

### 257 **Aggregation assay**

258 The diameter of a single TV particle was less than 0.1 µm (Oh et al., 2022b). Therefore, TV  
259 particles with a diameter larger than 0.1 µm were assumed to be aggregated TV particles in this

260 study. To quantify the TV aggregates with a diameter larger than 100  $\mu\text{m}$ , we employed the  
261 aggregation assay developed by (Oh et al., 2022b). In brief, the TV samples were passed  
262 through a 0.1  $\mu\text{m}$  syringe filter (Sartorius, Germany). The number of gene copies particles in  
263 the TV samples (i.e., total TV particles) and the filtrate (i.e., TV gene copies with a diameter  
264 less than 100  $\mu\text{m}$ ) were quantified using the RT-qPCR assays as described earlier. The  
265 aggregated virus particles were determined by subtracting the number of TV gene copies with  
266 a diameter of less than 100  $\mu\text{m}$  from the total TV particles.

267

### 268 **Statistical analysis**

269 Linear regression analyses were carried out to examine whether the influent TGEV RNA  
270 concentrations decreased over the experimental time frame (**Fig. S4**), as well as to investigate  
271 the effects of moringa protein concentrations on virus aggregation and inactivation (**Fig. 3**).  
272 Two-sample t-tests were performed to assess the quenching effects of FBS on the affinity of  
273 moringa proteins to viruses (**Fig. S5**), to evaluate the impact of moringa protein  
274 functionalization on virus removal efficacy of cotton filters (**Fig. 1**), and to compare the extent  
275 of virus aggregates detached from *MO*-cotton filters (**Fig. 2**). Mean-squared errors (MSE) were  
276 calculated to compare the goodness-of-fit of two non-linear regression models (the Thomas  
277 and logarithmic models), for TV removal kinetics (**Fig. S6**). All statistical analyses were  
278 conducted using OriginPro 2023.

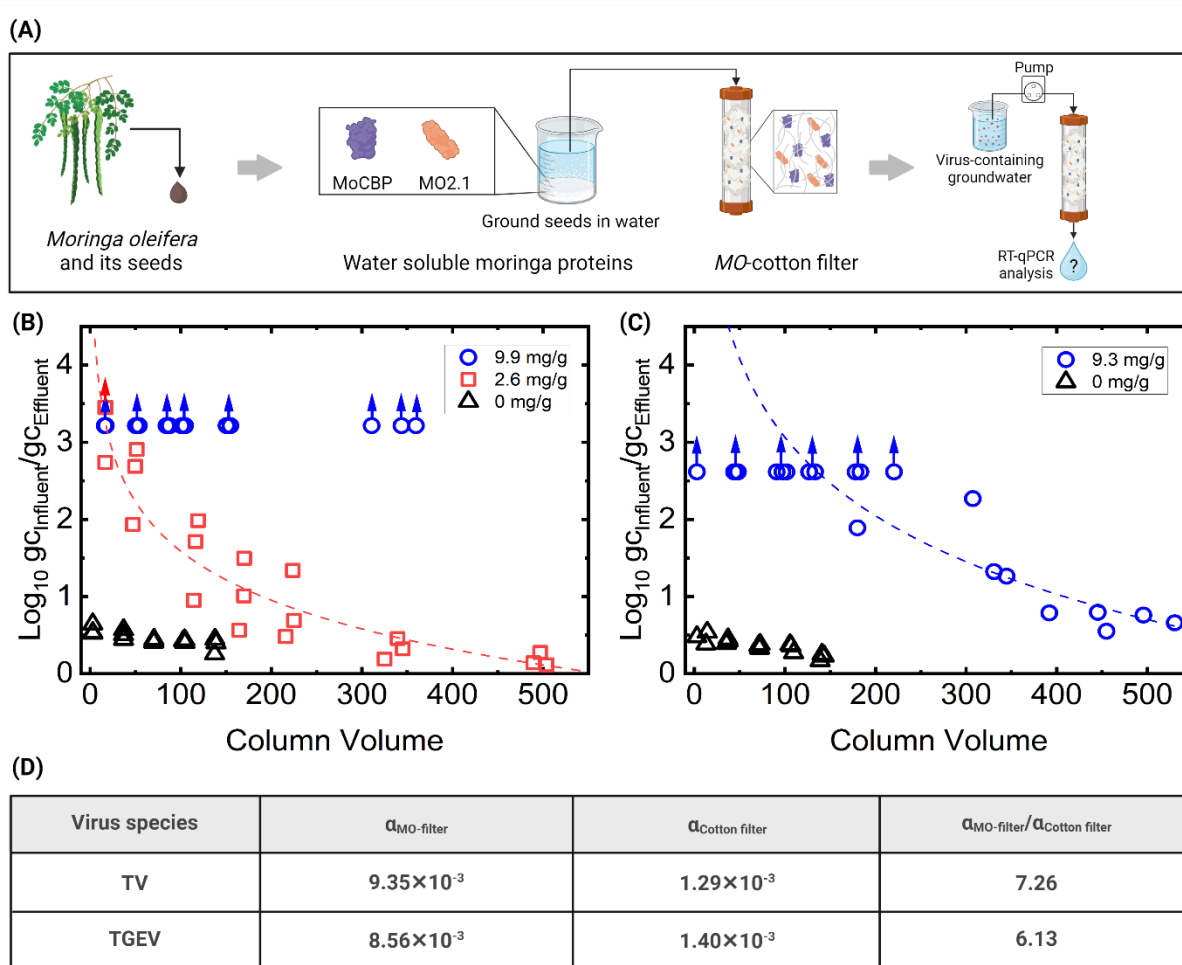
279

## 280 **Results**

### 281 **Moringa protein functionalized cotton filter can achieve 4-log virus reduction,** 282 **meeting regulations set by WHO and USEPA**

283 The TV removal efficacy of the *MO*-cotton filter is presented in **Fig. 1B**. When 9.9 mg/g of  
284 moringa protein was coated on the cotton fiber, the filter showed TV removal efficacy of

285 greater than  $3.2\text{-log}_{10}$  until 360 CV (blue circles in **Fig. 1B**). In contrast, cotton fibers without  
 286 moringa protein coating showed a maximum removal efficacy of less than  $0.6\text{-log}_{10}$  at the  
 287 beginning of the column experiment (i.e., 3 CV) which was significantly lower than that of the  
 288 cotton fiber with the 9.9 mg/g of moringa protein (two sample t-test;  $p < 0.001$ ). This finding  
 289 indicates that the significant increase in virus removal efficacy is attributed to the proteins of  
 290 the *MO* seed extracts.  
 291



292  
 293 **Fig. 1.** (A) Schematic illustrations for column experiments. (B) TV and (C) TGEV removal  
 294 kinetics were determined by column experiments with cotton fiber functionalized by water-  
 295 soluble moringa proteins. The symbols and lines represent measurements by RT-qPCR and  
 296 regression analysis by a logarithmic model, respectively. The legend on each figure indicates  
 297 the protein amount functionalized on the cotton filter. The arrows above symbols indicate that  
 298 the RNA concentrations of effluent were below the limit of detection. (D) Sticking coefficients  
 299 by a clean bed filtration model.  
 300

301           However, TV removal kinetics and the maximum TV removal efficacy of the filter were  
302 not determined by the filter with 9.9 mg/g of moringa protein because the virus concentrations  
303 in the effluent were all below the LOD for the entire period of the experiment. Therefore, we  
304 conducted another experiment with a reduced amount of moringa protein of 2.6 mg/g. The  
305 column with 2.6 mg/g of moringa protein showed a decrease in removal efficacy as the virus  
306 filtration progressed to 503 CV (red rectangles in **Fig. 1B**). We fitted data of virus removal  
307 efficacy, which were quantified by RT-qPCR (i.e., RNA concentrations of effluents were above  
308 the LOD), with two nonlinear regression models (the Thomas and logarithmic models) to  
309 understand virus removal kinetics and to estimate the maximum removal efficacy. We found  
310 that the logarithmic model described the virus removal kinetics better, showing 0.59 and 0.11  
311 of mean squared error (MSE) for TV and TGEV, respectively, compared to the Thomas model,  
312 which was 0.79 and 0.16 of MSE (**Fig. S6**). In particular, the differences in removal efficacy  
313 between the two models were more distinct at the beginning of the column experiment. For  
314 example, the TV removal efficacies at CV of 16 by the Thomas models were  $1.4\text{-log}_{10}$   
315 reduction, which was much lower than the experimental data,  $>3.2\text{-log}_{10}$  reduction (**Fig. S6**).  
316 Instead, we found that the logarithmic model estimated the virus removal efficacy at CV of 16  
317 to be  $3.3\text{-log}_{10}$  reduction (**Fig. S6**). With the logarithmic regression model, the maximum virus  
318 removal efficacy of the cotton filter with 2.6 mg/g of moringa protein was calculated to be  
319 higher than  $4\text{-log}_{10}$  reduction as a direct evaluation of this high removal efficiency was not  
320 possible because the concentration of viruses in the effluent samples was lower than the LOD  
321 of the RT-qPCR analysis. Based on these results obtained with a *MO*-cotton filter  
322 functionalized with 2.6 mg/g of protein, it can be concluded that the filter with enough moringa  
323 protein, such as 9.9 mg/g, would show virus removal efficacy of higher than  $4\text{-log}_{10}$  reduction.

324           We also evaluated TGEV removal by the *MO*-cotton filter because TGEV is an  
325 enveloped viral species that could show different behavior from non-enveloped viruses. First,

326 the TGEV removal efficacy of the filter with 9.3 mg/g of moringa protein was significantly  
327 higher than that of the cotton filter without the protein coating (t-test,  $p < 0.001$ ). This finding  
328 again supports that moringa protein is the key ingredient for TGEV removal. Next, the  
329 logarithmic model, excluding the data below the LOD, showed that the maximum TGEV  
330 removal efficacy was estimated to be higher than  $4\text{-log}_{10}$  until a CV of 67. Given the column  
331 experiments with the two different viral species in groundwater, the *MO*-cotton filters tested  
332 here have promising potential to meet the US EPA and WHO virus treatment requirements for  
333  $4\text{-log}_{10}$  reduction or inactivation of viruses <sup>29</sup>.

334 In addition to the kinetics models described above, clean bed filtration models have  
335 been widely used to calculate the sticking coefficient, a parameter evaluating the interaction  
336 between particles and filter media<sup>30,31</sup>. Based on the removal efficacies achieved by the *MO*-  
337 cotton filters at 350 CV (i.e., greater than  $3.2\text{-log}_{10}$  reduction for TV and  $1.2\text{-log}_{10}$  reduction  
338 for TGEV in **Fig. 1C**), the sticking coefficients for TV and TGEV to *MO*-cotton were  
339 calculated to be 7.3 and 6.1 times higher than those for cotton without *MO* functionalization,  
340 respectively. This result corroborates that the significant increase in virus removal efficacy is  
341 attributed to the *MO* proteins. Additionally, considering the experimental data and clean bed  
342 filtration theory, increasing the column heights to 7.5 cm and 19.6 cm (equivalent to a 24% and  
343 227% increase from the initial 6 cm) would achieve a 4-log reduction of TV and TGEV,  
344 respectively, at a CV of 350 (**Fig. 1D, Supplementary File**). It is important to note that the  
345 sticking coefficients shown here along with clean bed filtration models represent a widely  
346 established tool that can be used as a basis for design and optimization of filter size and  
347 operating flowrate for field-scale applications.

348

349 **Potential risk of infection due to virus detachment from the moringa protein**  
350 **functionalized cotton filter is negligible**

351 Even though *MO*-cotton filters show significant potential for removal of mammalian viruses  
352 from realistic water matrix, it is important to consider the risk of virus detachment during filter  
353 operation to ensure public safety. Viruses accumulated on the filter could be released back into  
354 the effluent<sup>32-34</sup> in situations when the virus concentration on the filter is higher than that of  
355 the influent or when the shear flow of groundwater disrupts the virus particles bound to the  
356 filter, resulting in the contamination of drinking water, as evidenced by previous studies<sup>35</sup>.  
357 Thus, we conducted virus detachment experiments after the virus removal experiment was  
358 completed to understand the potential virus detachment risk when using it for point-of-use  
359 drinking water purification.

360 First, we pumped sterilized groundwater without spiking viruses (i.e., no TV included)  
361 through the columns after the TV removal experiments (**Fig. 2A**) were completed to create  
362 conditions where the concentration of viruses was higher on the filter compared to the water  
363 matrix. The flow rate was 6 mL/min, three times faster than the influent flow rate of the virus  
364 removal experiment to ensure higher shear compared to normal operation. This experiment was  
365 conducted to simulate the possible virus detachment during the filter operation. TV RNA  
366 concentrations and infectious TV titers of the effluent are summarized in **Fig. 2B**. Note that the  
367 virus removal experiment with 0 mg/g of moringa proteins also showed a noticeable level of  
368 TV and TGEV removal efficacy (t-test;  $p < 0.001$ ), which was about 0.5- $\log_{10}$  reduction (**Fig.**  
369 **1**). This finding implies that cotton fibers itself (without moringa protein functionalization)  
370 contributed to trapping a portion of viruses from the groundwater. The effluent from the column  
371 with 0 mg/g of moringa protein contained infectious TV (**Fig. 2B**), which means that the  
372 binding between viruses and cotton is not strong enough to hold viruses from the shear flow of  
373 groundwater. On the other hand, the total TV RNA and infectious TV titer of the effluent from



374 the column with 9.9 mg/g of moringa proteins were not detected (**Fig. 2B**). Since this filter  
375 provided high removal efficacy of TV (i.g., higher than 3.2- $\log_{10}$  reduction) at the end of the  
376 removal experiment, there were available adsorption sites on moringa proteins where viruses  
377 are strongly attracted via electrostatic force over cotton fiber (blue circles in **Fig. 1B**). Thus,  
378 direct attachment to moringa proteins can prevent viruses from detachment due to the shear  
379 flow of groundwater. In the case of the column with 2.6 mg/g of moringa proteins, virus  
380 removal efficacy was reduced to values comparable to the column without moringa proteins at  
381 the end of the experiment (**Fig. 1B**). We detected infectious TV from the effluent, similar to  
382 the scenario of the column without moringa protein functionalization. The detection of  
383 infectious TV from this column can be explained by the fact that the available adsorption sites  
384 of moringa proteins were depleted in the column with 2.6 mg/g of moringa proteins, and thus  
385 a part of TV was loosely trapped on the cotton fiber.

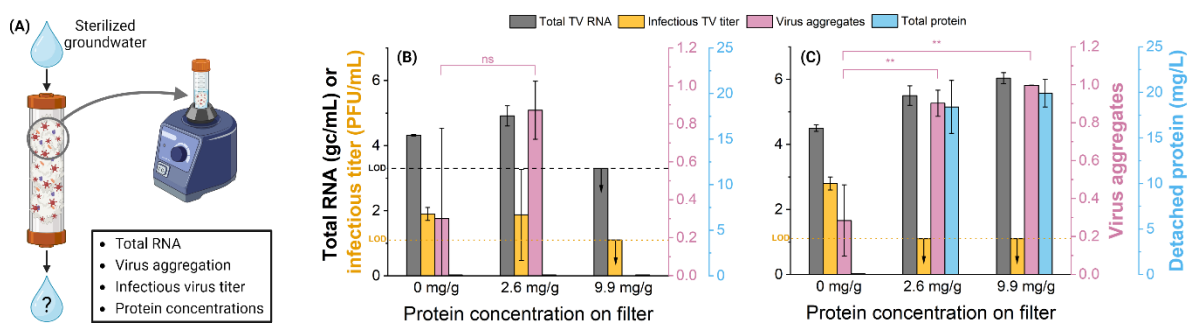
386 In another set of experiments, we forced viruses to detach from the filter by vortexing  
387 the a portion of the filter substrate with 10 mL molecular biology-grade water to simulate high  
388 shear conditions. This experiment was designed to demonstrate the possible maximum shear  
389 force by unexpected physical disruptions to the filter, such as instant injection of influent to the  
390 filter or external disturbances that could occur during daily use of a point-of-use filter.  
391 Vortexing cotton filter detached TV particles from all three columns with 0, 2.6, and 9.9 mg/g  
392 of moringa proteins (**Fig. 2C**), which indicates viruses could be detached by the shear force.  
393 However, interestingly, the detached viruses were infectious only when they were from the  
394 filter without moringa protein functionalization, whereas viruses were not infectious when they  
395 were from the columns with 2.6 and 9.9 mg/g of moringa proteins. The virus inactivation may  
396 be attributed to the moringa proteins also being detached from the filter by the shear force.  
397 Specifically, we detected proteins only from the two columns with 2.6 and 9.9 mg of moringa  
398 proteins. Also, the level of virus aggregates was significantly higher when moringa protein was

399 present in the extract (t-test;  $p < 0.001$ , **Fig. 2C**). Given the results from the detachment  
 400 experiments, we can conclude that the availability of adsorption sites of moringa proteins is  
 401 essential not only to achieve more than 4- $\log_{10}$  virus reduction but also to reduce the risk of the  
 402 potential release of viruses from the filter.

403

404

405



406 **Fig. 2.** (A) Schematic illustrations for detachment experiments. Results showing total TV RNA  
 407 concentration, infectious TV titer, virus aggregates (normalized to total RNA), and total protein  
 408 concentration in (A) the effluents of flowrate at 6 mL/min and (B) the extracts from cotton  
 409 vortexing (n=3). Two-sample tests were conducted for virus aggregate comparison (ns:  $p > 0.05$ ,  
 410 \*\*:  $p < 0.001$ ). Dashed and dotted lines indicate the limit of detection for total TV RNA  
 411 concentration and infectious TV titer, respectively. The downward arrows represent the true  
 412 values could be lower than the presented values.

413

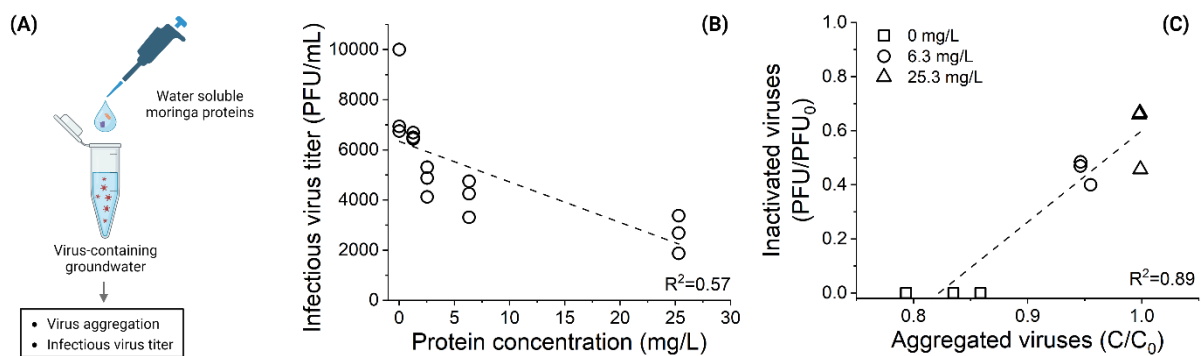
## 414 Electrostatic interactions drive the virus removal and subsequent inactivation if

### 415 detachment occurs due to high shear

416 Moringa proteins have been used as a coagulant that destabilizes contaminants by manipulating  
 417 charges of particles suspended in water<sup>36</sup>. To understand interactions between the moringa  
 418 proteins and viruses, we conducted batch experiments where the TV was incubated in varying  
 419 concentrations of the moringa proteins and analyzed levels of inactivated viruses and  
 420 aggregated viruses. **Fig. 3B** shows that the infectious TV titer significantly reduced as protein  
 421 concentration increased ( $p < 0.001$  from a linear regression analysis), indicating that the moringa  
 422 proteins potentially lead to virus inactivation. **Fig. 3C** represents the relationship between  
 423 levels of aggregated viruses and inactivated viruses after the reactions with the moringa

424 proteins. We found that the linear regression analysis shows the slope is significantly higher  
425 than zero ( $p < 0.001$ ), meaning virus aggregation could be related to virus inactivation. This  
426 analysis suggests that moringa proteins interact with TV, causing TV aggregation.  
427 Consequently, aggregation would likely prevent the TV from entering host cells, similar to how  
428 other plant-based extracts inactivate viruses (Oh et al., 2022b).

429



430

431 **Fig. 3.** (A) Schematic illustrations for batch experiment designed to mimic the interaction  
432 between water-soluble moringa proteins and TV in column effluent. (B) Infectious TV titer  
433 changes with total protein concentrations. (C) A relationship between levels of aggregated  
434 viruses and inactivated viruses after the reactions between TV and the moringa proteins were  
435 completed.

436

437 The strong affinity of the moringa proteins to viruses has been explored for filter media  
438 functionalization. Many studies appreciated natural cotton fiber as filter media because it  
439 provides high water permeability and its surface is easy to be functionalized<sup>16,37,38</sup>. Our  
440 previous study proved that cotton fiber is negatively charged (zeta potential of approximately  
441  $-20$  mV) in the pH range of 5–8, which allows for the adsorption of cationic moringa proteins,  
442 *Moringa oleifera* coagulant protein (MO2.1) and *Moringa oleifera* chitin binding protein  
443 (MoCBP), on the cotton fiber<sup>16</sup>. We confirmed the amount of protein saturated at the elapsed  
444 time of 17 minutes, showing that 6.7 mg/g of the maximum amount of the moringa proteins on  
445 cotton fiber when the protein concentration of the influent was 0.62 mg/mL (**Fig. S1**). Samineni  
446 et al. (2022) also found that the cationized cotton fiber attracted bacteriophage (MS2) via

447 electrostatic force, trapping them in the cotton filter. The moringa protein-functionalized cotton  
448 filter is also expected to remove TV and TGEV from the groundwater using similar  
449 mechanisms for the following reasons. First, the groundwater used in the current study  
450 contained 1.7 mM of calcium ions, and the pH was stable between 7.3 and 7.5 (**Table S3**, Shen  
451 et al., 2017). Second, isoelectric points (IEPs) of many enteric viruses are known to be below  
452 the pH of our groundwater. For example, IEPs of *caliciviridae*, such as norovirus and TV, were  
453 6.0<sup>40,41</sup> and 4.8<sup>42</sup>, respectively. In addition, SARS-CoV-2 and bovine coronavirus<sup>43</sup>, which  
454 are in *coronaviridae*, show IEP of 5.3 and 4.6, respectively. This low value of IEPs suggests  
455 that the TV and TGEV are negatively charged in our groundwater and electrostatically bind to  
456 the moringa protein functionalized filter.

457

## 458 **Discussion**

### 459 **Moringa protein functionalized cotton filter is a plausible point-of-use filter to reduce** 460 **the risk of virus infection in drinking water**

461 Although various water filtration technologies have been developed, only a few can  
462 successfully be applied for gravity-driven point-of-use filters for reducing the risk of virus  
463 infection to the level of drinking water because of the following two reasons. First, the  
464 successful point-of-use filter must demonstrate a 4-log<sub>10</sub> reduction or inactivation in pathogen  
465 concentrations (regulations by USEPA or WHO), over long periods of time to provide drinking  
466 water for daily use. Gutierrez et al. (2009) used a column (1.5 cm in diameter and 13.2 cm high)  
467 filled with hematite nanoparticle-coated glass fiber that removed rotavirus from actual  
468 groundwater (flowrate at 3 mL/min) by up to 4-log<sub>10</sub> reduction. However, its performance soon  
469 decreased to less than 3-log<sub>10</sub> reduction after 3-bed volumes (BV). Mthombeni et al. (2012)  
470 examined the use of resin beads coated with silver nanoparticles to deactivate microbes in  
471 drinking water in a column filtration system. *E. coli* containing water (2 mL/min) was flowed

472 through columns of 2 cm diameter and 30 cm length with silver nanoparticle-coated resin beads,  
473 and *E. coli* reduction efficacy was less than 1-log<sub>10</sub> after 30 CV. Our study supports that the  
474 *MO*-cotton filter can remove TV and TGEV by more than 4-log<sub>10</sub> reduction, which meets  
475 regulations by USEPA and WHO. Also, we experimentally confirmed that the filter achieved  
476 a 3-log<sub>10</sub> TV reduction of up to 300 CV, which is a noticeable period of efficient virus removal.  
477 Additionally, the size of the *MO*-cotton filters can be easily optimized as the materials required  
478 for fabrication are easily accessible and the method of fabrication is robust and scalable.

479         Second, the filter should not pose any risk of releasing harmful materials, which could  
480 be adsorbate (i.e., viruses) or adsorbent (i.e., filter media)<sup>32-34</sup>. For example, Chung et al. (2015)  
481 created hydrochar-amended sand beds (2.5 cm inner diameter and 10 cm bed height) and  
482 achieved a 2.4-log<sub>10</sub> removal of rotavirus and 2.4 for adenovirus up to 2 CV, but the viruses  
483 were released into the effluent at concentrations of 1% to 10% of initial concentrations when  
484 clean water was passed through it. In addition, the potential release of filter media could cause  
485 adverse impacts on human health. For example, release of nanomaterials from engineered filter  
486 medium could impact human health<sup>47,48</sup>. In this context, the moringa protein functionalized  
487 filter shows a minimal risk of infection by the viruses released from the filter as long as  
488 available adsorption sites of moringa proteins exist. Although we found that the moringa  
489 protein could be released from the filter by external physical force, the moringa proteins are  
490 considered safe for human health, and thus it has been used as a health supplement<sup>49,50</sup>, and  
491 the viruses accumulated on the moringa proteins were no longer infectious (**Fig. 2**). For the  
492 above two reasons, the functionalization of cotton filters with moringa protein could be a  
493 plausible point-of-use filter to reduce the risk of virus infection in drinking water.

494

495 **Moringa protein functionalized cotton filter is applicable to a wide range of drinking**  
496 **water sources**

497 Considering that virus adsorption to moringa proteins is the main removal mechanism, virus  
498 concentration in the influent will affect the removal efficacy of the moringa protein  
499 functionalized cotton filter. In this study, infectious virus titers in the influent groundwater  
500 were higher than  $10^3$  PFU/mL, which are likely much higher than those found in actual drinking  
501 water sources. For example, rotavirus concentrations in river water, treated wastewater, and  
502 untreated wastewater are reported to be  $10^{-3.0}$ ,  $10^{-2.2}$ , and  $10^{-1.3}$  focus-forming unit (FFU)/mL,  
503 respectively (Lodder et al., 2005; Rutjes et al., 2009). Given the findings that the moringa  
504 protein functionalized cotton filter functions properly with orders of higher virus  
505 concentrations, this filter is expected to reduce the risk of virus infection in actual water sources  
506 for a large number (estimated to be 1000s) of bed volumes.

507 In addition, organic matter has been reported to compete with adsorption sites of  
508 filtering systems with target contaminants<sup>51</sup>. We tested the performance of a filter using actual  
509 groundwater containing 1.6 mg/L of total organic carbon (TOC) (**Table S3**), a similar level to  
510 that found in typical groundwater used as a source of drinking water<sup>51-54</sup>. While groundwater  
511 is the most common form of self-supply in South Asia and Southeast Asia, rainwater collection  
512 is also prevalent in the Pacific<sup>55</sup>. Rainwater typically contains 2 mg/L or less of TOC<sup>56,57</sup>,  
513 indicating that the moringa protein functionalized cotton filter could also be effective in turning  
514 rainwater into safe drinking water.

515

516 **Moringa protein functionalized cotton filter is a plausible point-of-use filter for those**  
517 **with limited resources and under disaster or emergency scenarios**

518 The findings of this study provide valuable information for designing a point-of-use filter. The  
519 treated groundwater used in this study had a flow rate of 2 mL/min, which translates to a

520 superficial velocity of 0.7 m/h. If we increase the moringa protein functionalized cotton filter  
521 to 15 cm in diameter and 40 cm in height (1000 times increase in volume), the filter could  
522 provide 30 L of drinking water, a necessary amount of drinking water per day for a household  
523 <sup>58</sup>, just in 2.4 hours (i.e., 12.4 L/h capacity). Our experiments showed that the column can  
524 achieve a 3.2- $\log_{10}$  reduction or higher in TV until at least 350 CV, and this capacity is  
525 equivalent to 2545 L or 85 days of drinking water for a household. To construct a household-  
526 scale point-of-use filter, we would require 1.75 kg of cotton and 1 kg of moringa seeds, each  
527 of which costs approximately 5 US dollars or less in places where lack of access to centralized  
528 water supply systems <sup>59,60</sup>.

529         The filter fabrication and maintenance should be manageable by local people for  
530 sustainable operation. Various chemicals, such as zero-valent iron (ZVI) and magnesium oxide  
531 (MgO), have been proposed to functionalize filter media and improve virus removal efficiency  
532 <sup>61,62</sup>. The critical limitation of these chemicals is that they are not reusable and thus rarely  
533 applicable to the places with limited resources and disaster or emergency scenarios <sup>63,64</sup>.  
534 However, the moringa protein functionalized fiber filter is made of accessible natural materials  
535 (*Moringa oleifera* seeds and cotton fiber). This filter is also regenerable only with 600 mM  
536 NaCl and additional moringa proteins <sup>16</sup>. In addition, due to the high-water permeability of  
537 cotton filters, this filter does not require a pump to flow water through the filter.

538

## 539 **Conclusion**

540 We conducted systematic experiments under practically relevant conditions to determine virus  
541 removal efficacy and mechanisms of moringa protein functionalized cotton filter. Our  
542 experimental data clearly demonstrated that the moringa protein functionalized cotton filter can  
543 be used as a point-of-use filter to reduce the risk of virus infection to the level of drinking water.

544 In particular, this filter will contribute to providing clean drinking water to people in low- and  
545 middle-income countries.

546

## 547 **Acknowledgment**

548 This study was funded by the National Science Foundation (Award Number: 2023248).

549

## 550 **References**

- 551 1. WHO. Diarrhoeal disease. (2017).
- 552 2. Bouseettine, R., Hassou, N., Bessi, H. & Ennaji, M. M. Waterborne Transmission  
553 of Enteric Viruses and Their Impact on Public Health. *Emerging and*  
554 *Reemerging Viral Pathogens: Volume 1: Fundamental and Basic Virology*  
555 *Aspects of Human, Animal and Plant Pathogens* 907–932 (2020)  
556 doi:10.1016/B978-0-12-819400-3.00040-5.
- 557 3. Adelodun, B. *et al.* Assessment of socioeconomic inequality based on virus-  
558 contaminated water usage in developing countries: A review. *Environ Res* **192**,  
559 110309 (2021).
- 560 4. UNICEF. Pneumonia and diarrhoea: Tackling the deadliest diseases for the  
561 world's poorest children - UNICEF DATA. (2012).
- 562 5. Crider, Y. S., Tsuchiya, M., Mukundwa, M., Ray, I. & Pickering, A. J. Adoption of  
563 Point-of-Use Chlorination for Household Drinking Water Treatment: A  
564 Systematic Review. *Environ Health Perspect* **131**, (2023).
- 565 6. Sobsey, M. D., Stauber, C. E., Casanova, L. M., Brown, J. M. & Elliott, M. A. Point  
566 of Use Household Drinking Water Filtration: A Practical, Effective Solution for  
567 Providing Sustained Access to Safe Drinking Water in the Developing World.  
568 *Environ Sci Technol* **42**, 4261–4267 (2008).
- 569 7. Yang, H., Xu, S., Chitwood, D. E. & Wang, Y. Ceramic water filter for point-of-  
570 use water treatment in developing countries: Principles, challenges and  
571 opportunities. *Front Environ Sci Eng* **14**, 1–10 (2020).
- 572 8. Treacy, J. Drinking Water Treatment and Challenges in Developing Countries.  
573 *The Relevance of Hygiene to Health in Developing Countries* (2019)  
574 doi:10.5772/INTECHOPEN.80780.
- 575 9. Shirasaki, N., Matsushita, T., Matsui, Y. & Yamashita, R. Evaluation of the  
576 suitability of a plant virus, pepper mild mottle virus, as a surrogate of human  
577 enteric viruses for assessment of the efficacy of coagulation–rapid sand  
578 filtration to remove those viruses. *Water Res* **129**, 460–469 (2018).
- 579 10. Asami, T., Katayama, H., Torrey, J. R., Visvanathan, C. & Furumai, H. Evaluation  
580 of virus removal efficiency of coagulation-sedimentation and rapid sand  
581 filtration processes in a drinking water treatment plant in Bangkok, Thailand.  
582 *Water Res* **101**, 84–94 (2016).



- 583 11. Van der Laan, H. *et al.* Bacteria and virus removal effectiveness of ceramic pot  
584 filters with different silver applications in a long term experiment. *Water Res*  
585 **51**, 47–54 (2014).
- 586 12. Farrow, C., McBean, E. & Salsali, H. Virus removal efficiency of ceramic water  
587 filters: effects of bentonite turbidity. *Water Supply* **14**, 304–311 (2014).
- 588 13. Woodall, C. J. Waterborne diseases - What are the primary killers? *Desalination*  
589 **248**, 616–621 (2009).
- 590 14. Xiong, B. *et al.* Moringa oleifera f-sand Filters for Sustainable Water  
591 Purification. *Environ Sci Technol Lett* **5**, 38–42 (2018).
- 592 15. Samineni, L. *et al.* 7 Log Virus Removal in a Simple Functionalized Sand Filter.  
593 *Environ Sci Technol* **53**, 12706–12714 (2019).
- 594 16. Samineni, L. *et al.* Effective pathogen removal in sustainable natural fiber  
595 Moringa filters. *npj Clean Water* **2022 5:1** **5**, 1–12 (2022).
- 596 17. Samineni, L. *et al.* Highly effective nanoparticle removal in plant-based water  
597 filters. *Environmental Science: Advances* (2023) doi:10.1039/d3va00035d.
- 598 18. CDC. Norovirus | CDC. (2023).
- 599 19. Teunis, P. F. M. *et al.* Norwalk virus: How infectious is it? *J Med Virol* **80**, 1468–  
600 1476 (2008).
- 601 20. Tan, M. *et al.* Tulane virus recognizes sialic acids as cellular receptors. *Sci Rep* **5**,  
602 1–14 (2015).
- 603 21. Oh, C. *et al.* A novel approach to concentrate human and animal viruses from  
604 wastewater using receptors-conjugated magnetic beads. *Water Res* **212**,  
605 118112 (2022).
- 606 22. Bustin, S. A. *et al.* The MIQE Guidelines: Minimum Information for Publication  
607 of Quantitative Real-Time PCR Experiments. *Clin Chem* **55**, 611–622 (2009).
- 608 23. Han, R. *et al.* Adsorption of methylene blue by phoenix tree leaf powder in a  
609 fixed-bed column: experiments and prediction of breakthrough curves.  
610 *Desalination* **245**, 284–297 (2009).
- 611 24. Pisharody, L., Suresh, S. & Mukherji, S. Development and evaluation of DEAE  
612 silica gel columns for simultaneous concentration of coliphages and rotavirus  
613 from natural water samples. *Water Res* **203**, 117508 (2021).
- 614 25. Liu, X., Zhang, X. & Zhang, M. Major Factors Influencing the Efficacy of  
615 Vegetated Buffers on Sediment Trapping: A Review and Analysis. *J Environ Qual*  
616 **37**, 1667–1674 (2008).
- 617 26. Fulazzaky, M. A., Talaiekhosani, A. & Hadibarata, T. Calculation of optimal gas  
618 retention time using a logarithmic equation applied to a bio-trickling filter  
619 reactor for formaldehyde removal from synthetic contaminated air. *RSC Adv* **3**,  
620 5100–5107 (2013).
- 621 27. Green, A. W., DeSutter, T. M., Daigh, A. L. M. & Meehan, M. A. Wicking Salts  
622 from Brine-Contaminated Soils: A Potential Method for In Situ Remediation.  
623 *Agricultural & Environmental Letters* **4**, 180069 (2019).
- 624 28. Oh, C. *et al.* Inactivation Mechanism and Efficacy of Grape Seed Extract for  
625 Human Norovirus Surrogate. *Appl Environ Microbiol* **88**, (2022).
- 626 29. Surface Water Treatment Rule Documents | US EPA.  
627 <https://www.epa.gov/dwreginfo/surface-water-treatment-rule-documents>.

- 628 30. Logan, B. E., Jewett, D. G., Arnold, R. G., Bouwer, E. J. & O'Melia, C. R.  
629 Clarification of Clean-Bed Filtration Models. *Journal of Environmental*  
630 *Engineering* **121**, 869–873 (1995).
- 631 31. Tufenkji, N. & Elimelech, M. Correlation Equation for Predicting Single-Collector  
632 Efficiency in Physicochemical Filtration in Saturated Porous Media. *Environ Sci*  
633 *Technol* **38**, 529–536 (2004).
- 634 32. Auset, M., Keller, A. A., Brissaud, F. & Lazarova, V. Intermittent filtration of  
635 bacteria and colloids in porous media. *Water Resour Res* **41**, 1–13 (2005).
- 636 33. Bielefeldt, A. R., Kowalski, K. & Summers, R. S. Bacterial treatment  
637 effectiveness of point-of-use ceramic water filters. *Water Res* **43**, 3559–3565  
638 (2009).
- 639 34. Bichai, F., Dullemont, Y., Hijnen, W. & Barbeau, B. Predation and transport of  
640 persistent pathogens in GAC and slow sand filters: A threat to drinking water  
641 safety? *Water Res* **64**, 296–308 (2014).
- 642 35. Sen, T. K. & Khilar, K. C. Review on subsurface colloids and colloid-associated  
643 contaminant transport in saturated porous media. *Adv Colloid Interface Sci*  
644 **119**, 71–96 (2006).
- 645 36. Dorea, C. C. Use of *Moringa* spp. seeds for coagulation: a review of a  
646 sustainable option. *Water Supply* **6**, 219–227 (2006).
- 647 37. Ibrahim, H. M., Emam, E.-A. M., Tawfik, T. M. & El-Aref, A. T. Preparation of  
648 Cotton Gauze Coated with Carboxymethyl Chitosan and its Utilization for  
649 Water Filtration. *Journal of Textile and Apparel, Technology and Management*  
650 **11**, (2019).
- 651 38. De Respino, S., Samineni, L., Tu, Y. M., Oh, H. & Kumar, M. Simultaneous  
652 Removal of Oil and Bacteria in a Natural Fiber Filter. *Environ Sci Technol Lett* **9**,  
653 77–83 (2022).
- 654 39. Shen, Y. *et al.* Effect of Disinfectant Exposure on *Legionella pneumophila*  
655 Associated with Simulated Drinking Water Biofilms: Release, Inactivation, and  
656 Infectivity. *Environ Sci Technol* **51**, 2087–2095 (2017).
- 657 40. Goodridge, L., Goodridge, C., Wu, J., Griffiths, M. & Pawliszyn, J. Isoelectric  
658 Point Determination of Norovirus Virus-like Particles by Capillary Isoelectric  
659 Focusing with Whole Column Imaging Detection. *Anal Chem* **76**, 48–52 (2003).
- 660 41. Bolton, S. L. *et al.* Sanitizer efficacy against murine norovirus, a surrogate for  
661 human norovirus, on stainless steel surfaces when using three application  
662 methods. *Appl Environ Microbiol* **79**, 1368–1377 (2013).
- 663 42. Fuzawa, M., Bai, H., Shisler, J. L. & Nguyen, T. H. The basis of peracetic acid  
664 inactivation mechanisms for rotavirus and tulane virus under conditions  
665 relevant for vegetable sanitation. *Appl Environ Microbiol* **86**, (2020).
- 666 43. Christensen, E. & Myrmel, M. Coagulant residues' influence on virus  
667 enumeration as shown in a study on virus removal using aluminium, zirconium  
668 and chitosan. *J Water Health* **16**, 600–613 (2018).
- 669 44. Gutierrez, L. *et al.* Adsorption of rotavirus and bacteriophage MS2 using glass  
670 fiber coated with hematite nanoparticles. *Water Res* **43**, 5198–5208 (2009).
- 671 45. Mthombeni, N. H., Mpenyana-Monyatsi, L., Onyango, M. S. & Momba, M. N. B.  
672 Breakthrough analysis for water disinfection using silver nanoparticles coated  
673 resin beads in fixed-bed column. *J Hazard Mater* **217–218**, 133–140 (2012).

- 674 46. Chung, J. W., Foppen, J. W., Gerner, G., Krebs, R. & Lens, P. N. L. Removal of  
675 rotavirus and adenovirus from artificial ground water using hydrochar derived  
676 from sewage sludge. *J Appl Microbiol* **119**, 876–884 (2015).
- 677 47. Hao, L., Zhou, X. & Liu, J. Release of ZrO<sub>2</sub> nanoparticles from ZrO<sub>2</sub>/Polymer  
678 nanocomposite in wastewater treatment processes. *Journal of Environmental  
679 Sciences* **91**, 85–91 (2020).
- 680 48. Habibi Mohraz, M. *et al.* Assessment of the potential release of nanomaterials  
681 from electrospun nanofiber filter media. *NanoImpact* **19**, 100223 (2020).
- 682 49. García Milla, P., Peñalver, R., Nieto, G. & Trombetta, D. plants Health Benefits  
683 of Uses and Applications of Moringa oleifera in Bakery Products. (2021)  
684 doi:10.3390/plants10020.
- 685 50. Matic, I., Guidi, A., Kenzo, M., Mattei, M. & Galgani, A. Investigation of  
686 medicinal adietaryplantsreviewtraditionallysupplements:On  
687 moringausedoleiferaas. *J Public Health Afr* **9**, 191–199 (2018).
- 688 51. Hamidi, H. P., Kenari, S. L. D. & Basu, O. D. Simultaneous TOC and Ammonia  
689 Removal in Drinking-Water Biofilters: Influence of pH and Alkalinity. *Journal of  
690 Environmental Engineering* **146**, 04020080 (2020).
- 691 52. Stedmon, C. A. *et al.* A potential approach for monitoring drinking water  
692 quality from groundwater systems using organic matter fluorescence as an  
693 early warning for contamination events. *Water Res* **45**, 6030–6038 (2011).
- 694 53. Yang, F., Shi, B., Gu, J., Wang, D. & Yang, M. Morphological and  
695 physicochemical characteristics of iron corrosion scales formed under different  
696 water source histories in a drinking water distribution system. *Water Res* **46**,  
697 5423–5433 (2012).
- 698 54. Rizzo, L., Belgiorno, V. & Meriç, S. Organic THMs precursors removal from  
699 surface water with low TOC and high alkalinity by enhanced coagulation. *Water  
700 Supply* **4**, 103–111 (2004).
- 701 55. Foster, T. *et al.* Self-supplied drinking water in low- and middle-income  
702 countries in the Asia-Pacific. *npj Clean Water* 2021 4:1 **4**, 1–10 (2021).
- 703 56. Mattos, K. *et al.* Rainwater catchments in rural Alaska have the potential to  
704 produce high-quality water and high quantities of water for household use. *J  
705 Water Health* **17**, 788–800 (2019).
- 706 57. Huston, R., Chan, Y. C., Chapman, H., Gardner, T. & Shaw, G. Source  
707 apportionment of heavy metals and ionic contaminants in rainwater tanks in a  
708 subtropical urban area in Australia. *Water Res* **46**, 1121–1132 (2012).
- 709 58. WHO. Guidelines for drinking-water quality, 4th edition, incorporating the 1st  
710 addendum. (2017).
- 711 59. Kumar, Y., Thakur, T. K. & Thakur Antia. A Multifunctional Wonder Tree:  
712 Moringa oleifera Lam Open New Dimensions in Field of Agroforestry in India.  
713 *Int J Curr Microbiol Appl Sci* **6**, 229–235 (2017).
- 714 60. Voora, V., Bermudez, S., Farrell, J. J., Larrea, C. & Luna, E. Cotton prices and  
715 sustainability. *SUSTAINABLE COMMODITIES MARKETPLACE SERIES* (2023).
- 716 61. Michen, B., Fritsch, J., Aneziris, C. & Graule, T. Improved virus removal in  
717 ceramic depth filters modified with MgO. *Environ Sci Technol* **47**, 1526–1533  
718 (2013).

- 719  
720  
721  
722  
723  
724  
725  
726  
727  
728
62. Shi, C., Wei, J., Jin, Y., Kniel, K. E. & Chiu, P. C. Removal of viruses and bacteriophages from drinking water using zero-valent iron. *Sep Purif Technol* **84**, 72–78 (2012).
63. Uprety, S. *et al.* Assessment of microbial risks by characterization of *Escherichia coli* presence to analyze the public health risks from poor water quality in Nepal. *Int J Hyg Environ Health* **226**, 113484 (2020).
64. Uprety, S. *et al.* Microbial assessment of water, sanitation, and hygiene (WaSH) in temporary and permanent settlements two years after Nepal 2015 earthquake. *Science of The Total Environment* **877**, 162867 (2023).
- 729
- 730